Seasonal Changes of Sandbar Behavior in Nanwan Beach, South China

Article *in* Journal of Coastal Research · September 2008

Impact Factor: 0.98 · DOI: 10.2112/06-0773.1

Zhi-jun Dai
East China Normal University

Jinzhou Du
East China Normal University

Journal of Coastal Research	24	5	1209–1216	West Palm Beach, Florida	September 2008

Seasonal Changes of Sandbar Behavior in Nanwan Beach, South China

Zhi-Jun Dai†‡, Ji-Yu Chen†, Jin-Zhou Du†, and Chun-Chu Li‡

†State Key Lab of Estuarine & Coastal Research
East China Normal University
Shanghai, 200062, Peoples Republic of China
zjdai@sklec.ecnu.edu.cn

‡Institute of Estuarine and Coastal Research
Zhongshan University
GuangZhou, 510275, Peoples Republic of China

ABSTRACT

DAI, Z.-J.; CHEN, J.-Y.; DU, J.-Z., and LI, C.-C., 2008. Seasonal changes of sandbar behavior in Nanwan Beach, South China. *Journal of Coastal Research,* 24(5), 1209–1216. West Palm Beach (Florida), ISSN 0749-0208.

Frequent leveling data of beach profiles is collected from Nanwan Beach, which is characterized by a large seasonal variation in wave climate. Variability of the bar crest position obtained from the data of measured profiles is examined to quantify seasonal changes of the sandbar by empirical orthogonal function (EOF) analysis. The first eigenfunction showed that a rhythmic bar is a common feature of the beach all year round. The second eigenfunction effectively indicated that the two-dimensional variability of the bar behavior is of seasonal changes. The cross-shore bar movement ranged −30∼40 and −2∼60 m in summer and in winter, respectively. The next two eigenfunctions represented three-dimensional components of the bar behavior with a range of −21∼21 and −30∼21 m in summer and in winter, respectively.

ADDITIONAL INDEX WORDS: *Spatial and temporal variability, sandbar behavior, eigenfunction analysis.*

INTRODUCTION

Sandbar systems are significant reservoirs of sand and provide a natural defense mechanism for the coastline against erosion. The position and variability of these large-scale coastal geomorphology cells have important implications for short-time beach stability. Therefore, a quantitative investigation of morphologic bar changes is necessary for proper management of coastal resources, particularly in light of widespread coastal retreat.

Morphologically, sand bars display both linear and rhythmic features (GREENWOOD and DAVIDSON-ARNOTT, 1979a, 1979b; SHORT, 1975, 1979; Wright *et al.,* 1979) that reflect alongshore invariability (linear or two-dimensional [2-D]) characters and alongshore nonuniform (three-dimensional [3-D]) characters (LIPPMANN and HOLMAN, 1990). As these features exhibit the spatial and temporal variability of sandbar behavior, many coastal researchers have investigated the change and formation of these characteristics (GREENWOOD and DAVIDSON-ARNOTT, 1979a; MOORE, SULLIVAN, and AUBREY, 2003; SHORT, 1975, 1979; WRIGHT *et al.,* 1979). Commonly, sandbars orient parallel to the shore and locate where the water depth is less than 8 m, and alongshore multiple sandbars are often found in the nearshore zone (RUESSINK and TERWINDT, 2000). If more than one bar is rhythmic, the outer bar has the larger rhythmic wave length (GREENWOOD and DAVIDSON-ARNOTT, 1979a). Earlier, some authors had devised conceptual equilibrium models for linear bar formation on the basis of the plunging processes of incident waves (KEULEGAN, 1948), the shoaling and breaking regions of incident waves (GREENWOOD and DAVIDSON-ARNOTT, 1979a), and the anti-node or nodal location of waves standing in the cross-shore such as reflected incident waves (BOWEN, 1980; CARTER, LIU, and MEI, 1973; LAU and TRAVIS, 1973; SHORT, 1975) or progressive edge waves (BOWEN, 1980). Other equilibrium models had also been proposed for the generation of 3-D or crescentic bar forms (BOWEN and INMAN, 1971; HOLMAN and BOWEN, 1982). As sandbars provide natural protection by dissipating wave energy, it is important to make long-term or short-term predictions of their behavior. With the development of surveying techniques, presently, most researchers investigate the bar behavior by means of digital video cameras (HOLLAND *et al.,* 1997; VAN ENCKEVORT and RUESSINK, 2001a, 2001b, 2003). The digital video techniques to survey sandbars depend on incident wave breaking. The preferred wave breaking over the shallows of the bar, which represent the bar crest, results in a sharp contrast between the bar and the trough region (RUESSINK, VAN ENCKEVORT, and AARNINKHOF, 2002). Therefore, it can be reasonable to obtain the value of the bar position. However, the use of the digital camera will be limited as follows: (1) a wave cannot break over the site while the wave height is considerably small; (2) a foggy day also influences the use of the digital camera; (3) when a wave breaks over the bar crest, the spray region is too big to distinguish the actual site of bar crest. In such case, traditional surveying techniques such as leveling may be better to identify the bar crest. Thus, to further understand sandbar behavior, data on the position of sandbars

DOI: 10.2112/06-0773.1 received 4 October 2006; accepted in revision 8 May 2007.

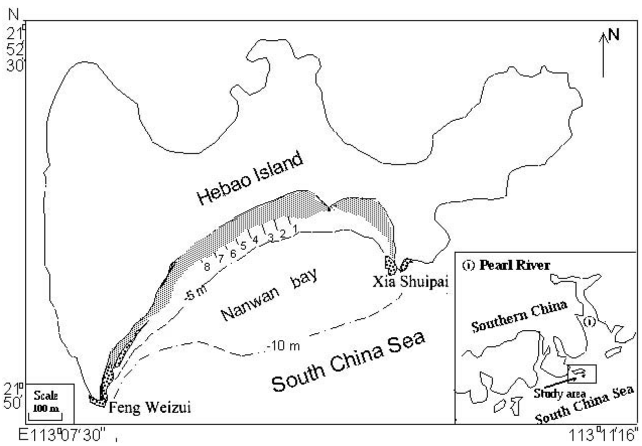

Figure 1. Location map and profile stations for Nanwan Beach of Hebao Island in South China.

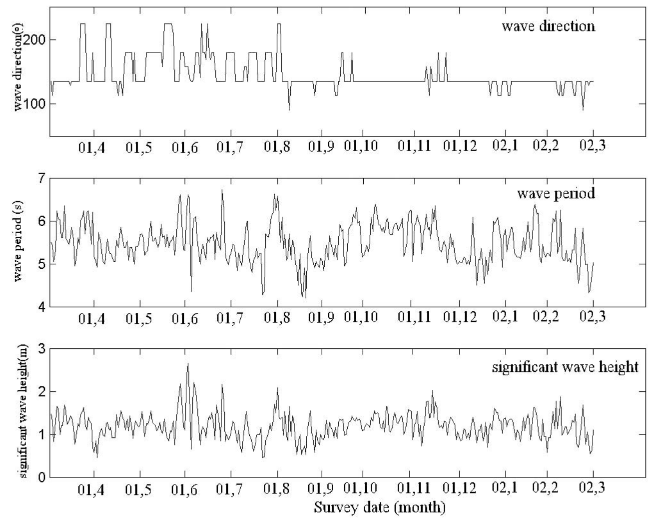

Figure 2. Records of wave parameters from April 2001 to March 2002.

in this paper were collected by using a traditional leveling technique. On the basis of the leveling of the beach profiles in South China, the purpose of this paper is to quantify the morphologic changes of these sandbars in different seasons using empirical eigenfunction analysis (EOF), which has been successfully used to describe variations in profile configuration (BOWMAN, 1981; MUNOZ-PEREZ, MEDINA, and TEJEDOR, 2001; WIJNBERG and TERWINDT, 1995; WINANT, INMAN, and NORDSTOTORM, 1975). The advantage of EOF is that a set of intercorrelated variables can be decomposed into a set of statistically independent variables. The new variables are linear combinations of the original variables but mutually orthogonal. Eigenanalysis separates the temporal and spatial dependence of the data, representing data as a linear combination of products of corresponding functions of time and space. However, the result of bar behavior obtained by EOF analysis is affected, as the bar position is difficult to survey in certain natural conditions (*i.e.,* foggy). Occasional missing estimates of the bar position are interpolated in the following manner (LIPPMANN and HOLMAN, 1990):

$$x(y_i, t_j) = x(y_i, t_{j-1}) + [\bar{x}(t_j) - \bar{x}(t_{j-1})] \tag{1}$$

where $x(y_i, t_j)$ is the bar crest position state at point i and time j, $\bar{x}(t_j)$ denotes the longshore mean at time j. That is, the interpolated value of $x(y_i, t_j)$ at a location is just sum of the previous value $x(y_i, t_{j-1})$ at that location plus the changed value $[\bar{x}(t_j) - \bar{x}(t_{j-1})]$ in the mean bar position over the time between adjacent samples.

After the above-mentioned values were obtained, they can be added into following formula (WALLACE, 1972):

$$x(y, t) \approx \sum_{j=1}^{p} a_j(t)e_j(y) = a_1(t)e_1(y) + \sum_{j=2}^{p} a_j(t)e_j(y) \tag{2}$$

where $e_j(y)$ are the spatial eigenfunctions and $a_j(t)$ are the corresponding amplitude temporal eigenfunctions. p is the number of eigenfunctions in the series. A linear factor, $e_1(y)$, represents the sample mean bar position, and the corresponding amplitude time series, $a_1(t)$, expresses a quantified amplitude of the bar alongshore. The remaining spatial factors of the second term in Equation (2) represent the 2-D and 3-D bar structure and have a collective variance, $V(t)$, which is defined by (LIPPMANN and HOLMAN, 1990; WALLACE, 1972)

$$V(t) = \sum_{y} \left[\sum_{j=2}^{p} a_j(t)e_j(y)\right]^2 \tag{3}$$

Therefore, the degree of cross-shore and longshore variability of the bar crest can be quantified by Equation (3). It should be noted that the series $V(t)$ in Equation (3) has been truncated at p significant factors to reduce the effect of noise in the analysis (WALLACE, 1972).

On the basis of the mentioned equations above, in the present paper, the bar crest position data is restructured and transformed by eigenfunction analysis.

REGIONAL SETTING

The studied region is in Nanwan Bay Beach (4 km length, 21°51′N, 113°09′E), South China. The beach is tied between bedrock headlands at Xia Shui-pai point and Feng Wei-zui point (Figure 1). The bay bathymetric lines between the two headland outcrops are parallel to the shoreline. The appearance of the beach is gently arc-shaped. The morphology of inshore and foreshore beach is linked with the nearshore water circulation pattern, and the beach exhibits the full range of morphologic states described for New South Wales beaches by Wright et al. (1979). Moreover, alongshore multibar patterns are common on the central zone of the beach, and terrace shoals occur on the eastern rockwall section of the beach.

Monsoons control the climate in this region (DAI, LI, and ZHANG, 2004). The wave climate is dominated by a highly variable wind–wave climate superimposed on persistent high-energy, south to southeasterly swell. Figure 2 contains a summary of the basic wave parameters that have been col-

Table 1. *Mean position of the bar crest.*

Profile	1	2	3	4	5	6	7	8
Distance to the stake (m) (summer)	106.14	95.59	98.83	94.73	84.73	86.58	84.86	96.61
Distance to the stake (m) (winter)			105.89	126.89	127.75	122.33	149.46	149.75

lected from the buoy located ~40 km SE of the study site (Figure 1). The mean wave height of 1 m usually occurs in this region. The waves are S-SSW during May to September and S-SE during October to March (Yang *et al.,* 1995). The late summer months are characterized by a more variable wave pattern in which NE winds prevail. Thus, the wave and wind conditions of March and July are typical of winter and summer, respectively, in this region. Tides are semidiurnal and vary in a range from neaps of 0.2 m to springs of 2.1 m.

DATA COLLECTION AND RESEARCH METHODS

Field data were collected during July 7 to August 24 (summer), 2001 and February 24 to March 28 (winter), 2002. The daily topographic surveys were made by using the stake and adoptive traditional leveling technique on the central section of the beach located in an area exposed to the prevailing southeasterly swell (Emery, 1961). This section longitudinally expanded 350 m, which was equally divided by a series of eight shore-normal stake-signed profiles, and transversally expanded about 200 m from the stake to the beachline with a water depth of about 3 m. Meanwhile, survey data relate to a common datum (Yellow Sea Height Datum in China). Because of the need of the coastal engineering and several typhoon actions in this zone in summer, all the stakes of the beach were established again in winter at a location approximately 200 m west from previous surveys.

In this study, a bar was treated as the perturbation to an underlying smooth profile, and a value of the perturbation position was obtained as $x(y, t)$, where t is time and y is the perturbation longshore position of each profile. Occasional missing estimates of the bar position occur in certain natural conditions; the bar position is obtained by Equation (1) (Lippmann and Holman, 1990).

The nearest perturbation position on each daily profile, where the distance of its position is the shortest of all of the perturbation positions of each profile to the shoreline, is calculated by inputting data to the EOF analysis. The seasonal behavior is characterized by Equations (2) and (3).

RESULTS AND DISCUSSION

Position and Occurrence Frequency of the Sandbars

The mean position alongshore is listed in Table 1 and shown in Figure 3. In combination with the measured data and field survey, differences of the main distribution of the bar in summer and in winter show that: (1) as the wave frequently broke over the nearshore region, most of the sandbars in summer distribute within the range from the shoreline to about 100 m offshore, with the height of the bar crest from −1 to 0 m. However, the bar in winter occurred over 100 m to the shoreline for the breaking position of the wave is offshore, and the height of the bar crest is below −1 m. (2) The occurrence frequency of the multiple bar in summer is much higher than that in winter. (3) Clearly, the distribution of the sandbars is seasonal, with the bar occupying the nearshore region in summer and offshore region in winter. The seasonal cycle phenomena were also observed in several published works (Aubrey and Ross, 1985; Birkemier, 1985).

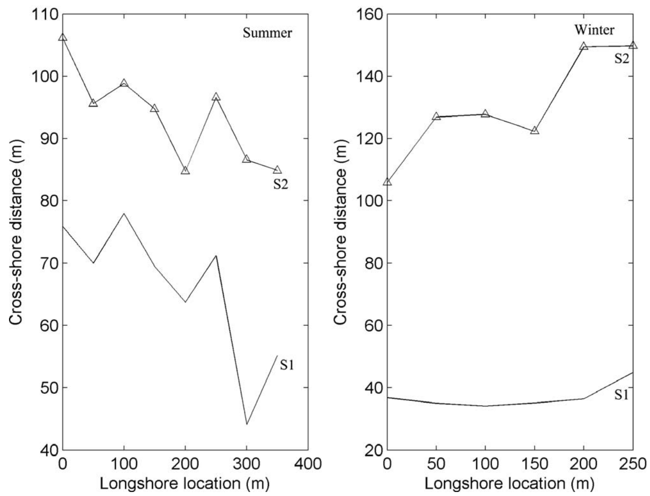

Figure 3. The mean position of the isobath 0 meter (S1) and the mean position of the bar crest (S2) longshore in summer and winter.

Longshore Structure in Sandbar Crest Position

On the basis of the common datum, the mean isobath 0 meter (S1) and the mean bar crest position (S2) calculated in summer and in winter are respectively shown in Figure 3. Obviously, the mean bar crest position is reasonably parallel to isobath 0 meter position and is located between a range of 80 m to 110 m offshore in summer, and of 100 m to 150 m offshore in winter. It is seen in Figure 3 that various tendencies of the bar position against isobath 0 meter position are accordant both in summer and in winter. Therefore, the mean bar crest position may have some relationship with the isobath 0 meter position, as illustrated in Figure 4. The high linear correlation ($r = 0.8024$ in summer and $r = 0.5287$ in winter) represents the retreat and advance of the shoreline closely related to the changes of the sandbar. This correlation can be also evidenced by the t test that has been applied in statistical analysis in geoscience (Barnett, 1983; Solow, 1987). The results also indicate that both cyclic behavior of the bar and accretion/erosion of the beach were associated with sediment transport (Aubrey and Ross, 1985).

Eigenfunction Analysis

The results of eigenfunction analysis from the bar crest position data are summarized in Table 2. The functions of $\sum_{j=1}^{p} a_j(t)e_j(y)$ of Equation (2) are ranked according to the per-

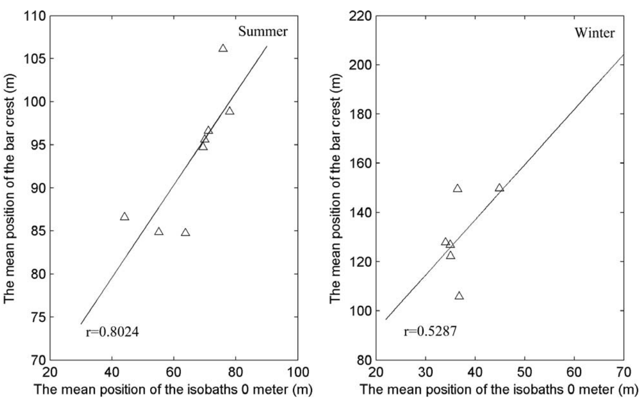

Figure 4. The correlation between the mean position of the isobath 0 meter and the mean position of the bar crest longshore in summer and winter.

centages of the mean square value of the data. These percentages are accounted for by each function, and enable evaluation of the relative importance of each function in explaining the observed bar variability (SHENOI, MURTY, and VEERAYYA, 1987). Since four functions in Table 2 account for more than 98% of the total mean-square value, emphasis is placed on them. To express the changes of the sandbar crest position directly, the sample mean has not been removed from the data set initially. Figures 5 and 6 show the decomposition of the bar crest data into the first four orthogonal EOFs (Equation [2]). The high EOFs calculated by Equation (2) were deleted since high EOFs were generally associated with field sampling errors (WINANT, INMAN, and NORDSTOTORM, 1975).

First Eigenfunction (Mean Position of the Bar Crest Function)

The first eigenfunction accounts for 95.45% in summer and 96.88% in winter of the mean square value of the surface fluctuations (Table 2). This eigenfunction shows the mean position of the bar crest and similarity in its shape for bar structure in different seasons (Figures 5 and 6). Both mean position and similarity provide information on bar structure alongshore. As far as the mean position of the bar crest is concerned (Figure 3), the curves of $e_1(y)$ in Figure 5A and in Figure 6A are not only similar in the mean position of the bar crest, but approximately sinusoidal. In addition, by contrast with the first spatial eigenfunction of the bar crest in winter, bar structure is more rhythmic and has more frequent changes in summer because of several typhoons affecting this region (DAI *et al.,* 2007). This shows that rhythmic bar could be common bar morphology along Nanwan Beach and especially tends to occur in response to the typhoon action. In comparison with a picture taken on July 7, 2001 (Figure 7), it is interesting that the rhythmic bar becomes more easy to observe in a picture taken after a typhoon on July 10, 2001 (Figure 8). However, the linear bar was relatively easy to identify under all wave conditions in previous work by image-processing technique (LIPPMANN and HOLMAN, 1990). Their observations suggest that linear bars tend to occur ex-

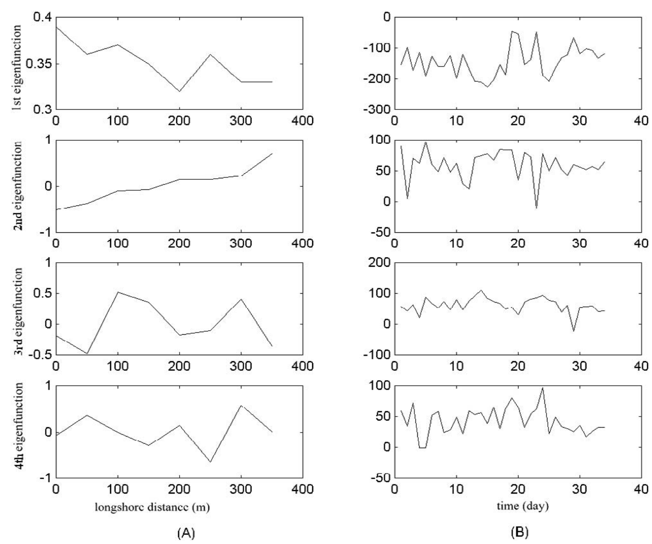

Figure 5. Spatial and temporal dependence of the eigenfunctions of the position of the bar crest data sets in summer.

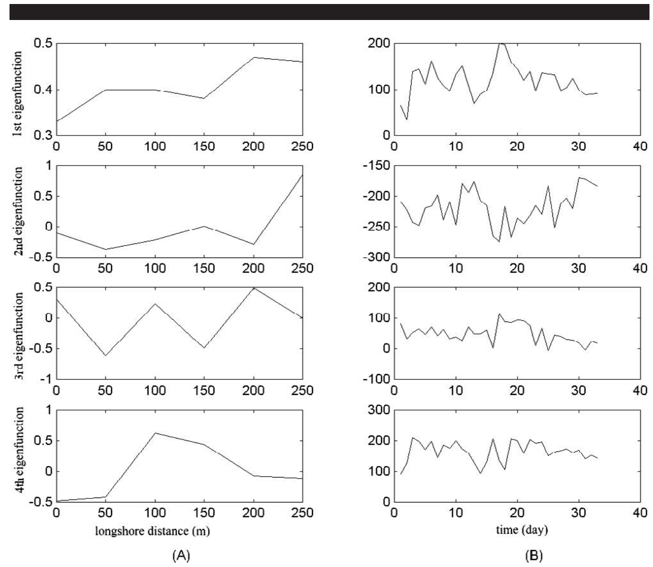

Figure 6. Spatial and temporal dependence of the eigenfunctions on the position of the bar crest data sets in winter.

Table 2. *Percentage of the mean-square value of the data explained by the first four eigenfunctions and the percentage variance of the demeaned data set accounted by the values in brackets.*

Survey site	1st function	2nd function	3rd function	4th function
Bar position in summer	95.47	1.29 (28.73)	1.03 (22.9)	0.821 (18.2)
Bar position in winter	96.88	1.39 (44.64)	0.59 (19.11)	0.57 (18.24)

Figure 7. Longshore bar types (photo taken on 7 July 2001).

clusively during storm periods. As the breaking position of the incident wave in the crest of a linear bar or in a rhythmic bar may be identical, especially to the high-energy events, these two bar types could not be distinguished from the processed exposure images. Thus, rhythmic bar types could be attributed into linear bars from high-energy events. The different type of bar observed in response to the typhoon action between us and LIPPMANN and HOLMAN (1990) may result from the different field sampling methods.

Second Eigenfunction

The second eigenfunction accounts for 1.29% and 1.39% of the total bar variability in summer and winter respectively, and also 28.73% and 44.64% of the residual variance from the mean bar crest position function (Table 2). $e_2(y)$ is approximately linear in summer and light sinusoidal in winter, clearly expressing the mean cross-shore location of the bar. The corresponding $a_2(t)$ represents the time dependence of the 2-D (linear) morphologic component, and can contain some uncertain short-time cycles for the cross-shore movement of the bar (Figures 5B and 6B). This phenomenon is similar to the 2-year variability in bar position (LIPPMANN and HOLMAN, 1990). However, on the basis of Equation 3 ($p = 2$), variability in bar position denotes cross-shore bar migration in summer, with a range of mean on-offshore bar movement of $-30{\sim}40$ m, and variability of the bar in winter represents cross-shore bar migration (44.64% variance associated with the second eigenfunction), with a range of mean on-offshore bar movement of $-2{\sim}60$ m. Obviously, combining the above analysis with the measured wave data (Figure 2), 2-D variability of the bar is an unimportant component of the total behavior changes of the bar in summer, which resulted from an easily shifted wave incidence direction (Figure 9). The cross-shore movement of the bar can dominate main behavior of the bar in winter because of prevailing ES wave effecting the migration of the bar (Figure 10). Obviously, the result corresponds to previous studies (GREENWOOD and DAVIDSON-ARNOTT, 1979a, 1979b; SHORT, 1979; SUNAMURA, 1988; WRIGHT *et al.,* 1979; WRIGHT and SHORT, 1984) in which cross-shore movement of the bar was associated with the local wave condition. However, several of them had only a focus on the prediction of the bar movement on the basis of the evolved sequence of bar states, and they were to analyze the position of the nearshore bar using only one single profile or based primarily on visual observations. These methods may indicate that the bar behavior was qualitatively char-

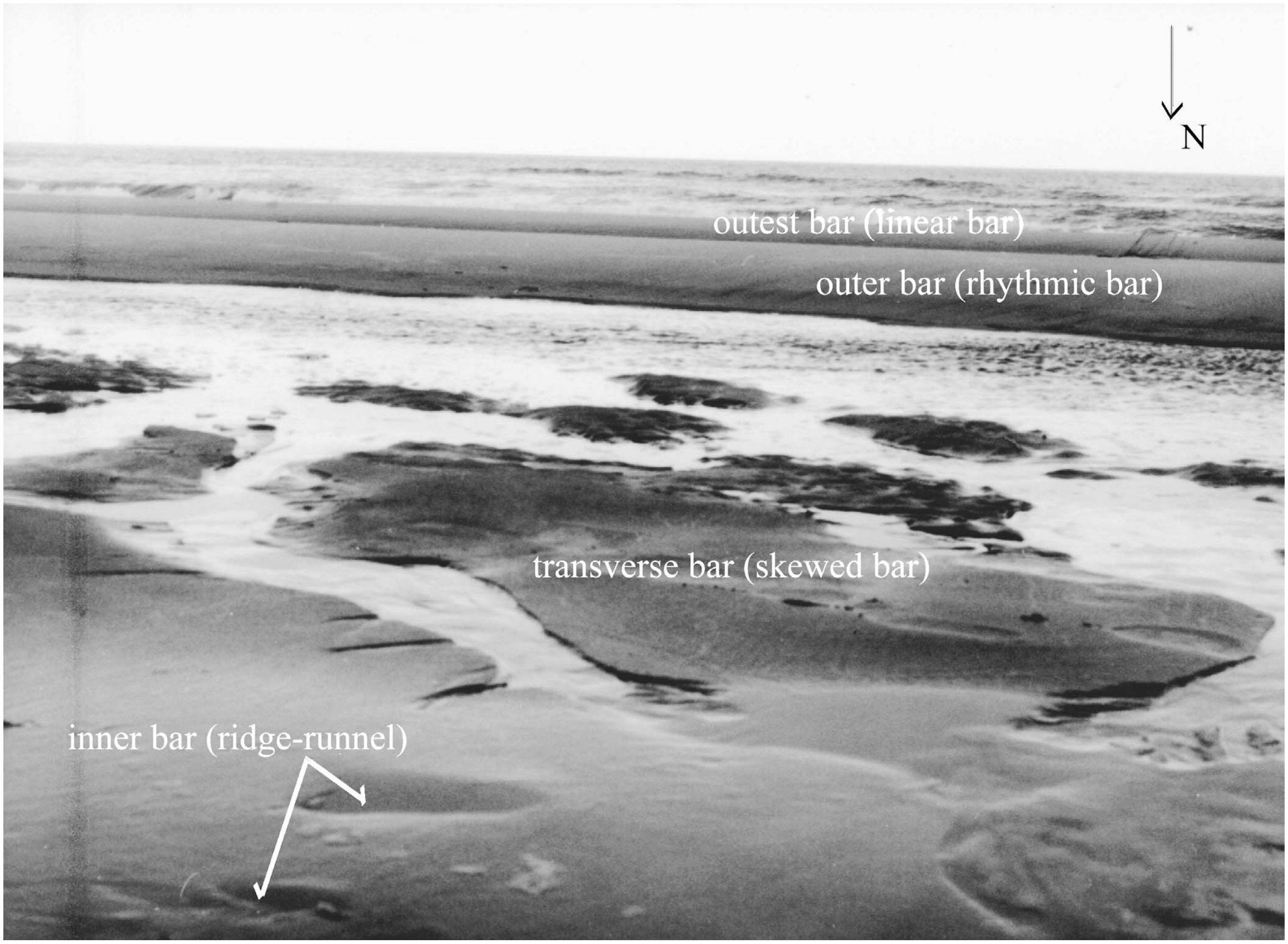

Figure 8. Longshore bar types (photo taken on 10 July 2001).

acterized. Although variability of bar was quantitatively expressed, the timescale was only limited to yearly intervals (LIPPMANN and HOLMAN, 1990). In the present paper, the results present that movement of the bar could be quantified and have a detailed span that varied with the changes of wave climates in a seasonal timescale.

Remaining Eigenfunction

The next two EOFs represent 3-D variability in bar crest position (LIPPMANN and HOLMAN, 1990) and account for 41.1% and 37.35% of the residual variance in summer and winter, respectively (Table 2). The spatial configuration of the two EOFs shows similar patterns in summer and in winter (Figures 5 and 6). These patterns appear somewhat sinusoidal, and contain the shift of different bar types. Field research in the present paper indicates that rhythmic bar, transverse bar, ridge-runnel, and longshore bar-trough often occur simultaneously on Nanwan Beach and converted into each other. For example, Figure 7 shows that both a rhythmic bar (inner bar) and longshore bar-trough (outer bar) types existed on the beach, but changed to a transverse bar type on July 10, 2001 (Figure 8). Although previous studies discussed the equilibrium models of bar types and associated cyclic sequential models, it was not mentioned that different bar types can be simultaneous observed at the same time (DAI, 2003). In addition, longshore variability associated with the 3-D component in bar position in the present work was calculated by means of Equation 3 ($j = 3$, $p = 4$). Therefore, the resulting variance time series, $V(t)$, can express the evolution of longshore variability. The obtained $V(t)$ may show bar variability with a range of longshore bar migration with its value of $-21\sim21$ m in summer and $-30\sim21$ m in winter, respectively.

CONCLUSIONS

Using EOFs, the behavioral patterns of the sandbars in different seasons were analyzed along the central zone of Nanwan Beach, Hebao Island, South China. The results are summarized as:

(1) The mean position of isobath 0 meter and the mean bar

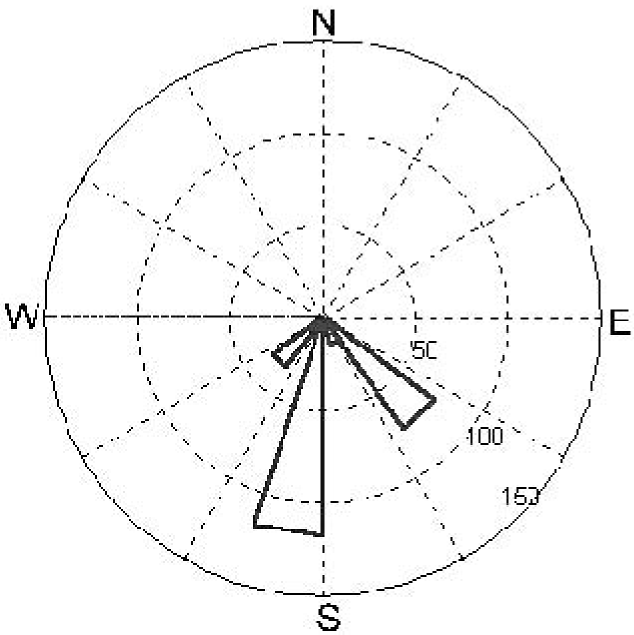

Figure 9. Frequency and incidence direction of the wave from June to July, 2001.

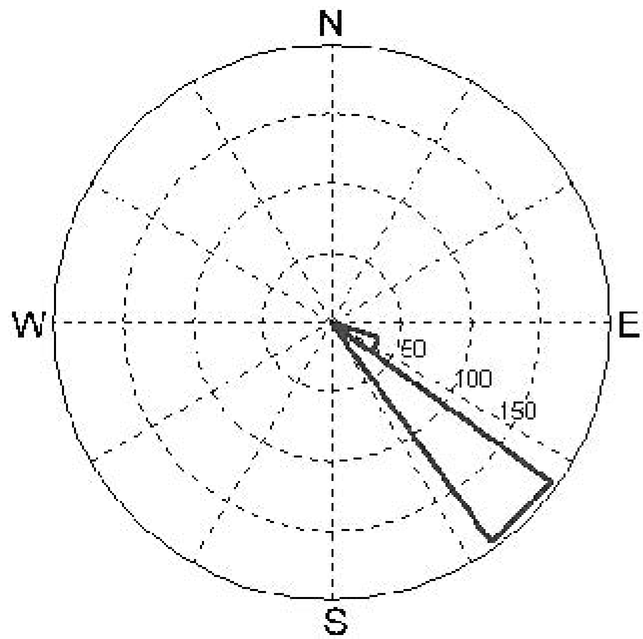

Figure 10. Frequency and incidence direction of the wave from February to March, 2002.

position are closely correlated. Cyclical pattern in erosion and accretion of the beach can be expressed by the retreat and advance of the bar position.

(2) The first eigenfunction represents the mean bar position, which has an obvious rhythmical variation. This function accounts for more than 95% of the variability of the sandbar behavior in summer and in winter, respectively, which demonstrate that the rhythmic bar type is the common bar form occurring both in summer and winter at Nanwan Beach.

(3) The 2-D variability of the bar is represented by the second eigenfunction. Cross-shore bar migration dominates bar variability in winter, accounting for 44.64%, with a range of −2∼60 m. However, 2-D variability of the bar migration plays a minor part of the bar behavior in summer, accounting for 28.73%, with a range of −30∼41 m.

(4) The third and fourth eigenfunctions represent 3-D variability of the bar. It shows that longshore bar variability in summer is dominant (accounting for 41.1%), and the resulting time series indicate the bar migration with a range of −21∼21m. However, the same variable frequency as the 3-D variability of the bar (accounting for 37.35%) in winter has a range of −30∼21m.

ACKNOWLEDGMENTS

This study was supported by National Science Foundation in China (grant no. 40506021, 40771200), The Shanghai Youth Science and Technology Venus and Pujiang Program (grant nos. 06QA14016 and 06PJ14031), and Guangdong Province Nature Fund Committee (grant no. 011181). Thanks are also given to our colleagues Shi-jun Wang and Hu-da for their field work.

LITERATURE CITED

Aubrey, D.G. and Ross, R.M., 1985. The quantitative description of beach cycles. *Marine Geology,* 69, 155–170.

Barnett, T.P., 1983. Interaction of the monsoon and Pacific trade wind systems at interannual time scales, part 1: the equatorial zone. *Monthly Weather Review,* 111, 756–733.

Birkemier, W.A., 1985. Time scales of nearshore profile chane. *In: Proceedings of the 19th International Conference on Coastal Engineering* (New York, American Society of Civil Engineers), pp. 1507–1521.

Bowen, A.J., 1980. Simple models of nearshore sedimentation: beach profiles and longshore bars, coastline of Canada. Littoral processes and shore morphology. *Geology Survey Canada,* 1–11, 80–100.

Bowen, A.J. and Inman, D.L., 1971. Edge waves and crescentic bars. *Journal of Geophysical Research,* 76, 8662–8671.

Bowman, D., 1981. Efficiency of eigenfunctions for discriminant analysis of subaerial non-tidal beach profiles. *Marine Geology,* 39, 243–258.

Carter, T.G.; Liu, P.L., and Mei, C.C., 1973. Mass transport by waves and offshore sand bedforms. *Journal of Waterway Harbors Coastal Engineering Division,* American Society Civil Engineering, WW2, 165–184.

Dai, Z.J., 2003. Types, Models of the Arc-Shaped Coast and Associated Beach Processes, South China. Guangzhou, China: Zhongshan University, Doctoral thesis, pp. 210–225 (in Chinese with English abstract).

Dai, Z.J.; Du, J.Z.; Li, C.C., and Chen, Z.S., 2007. The configuration of equilibrium beach profile in South China. *Geomorphology,* 86, 441–454.

Dai, Z.J.; Li, C.C., and Zhang, Q.L., 2004. Fractal analysis on shoreline patterns for the crenulate-bay beaches, Southern China. *Estuarine, Coastal and Shelf Science,* 61(1), 65–71.

Emery, K.O., 1961. A simple method of measuring beach profiles. *Limnology and Oceanography,* 6, 90–93.

Greenwood, B. and Davidson-Arnott, R.G.D., 1979a. Sedimentation and equilibrium in wave-formed bars: a review and case studies. *Canada Journal of Earth Science,*16, 313–332.

Greenwood, B. and Davidson-Arnott, R.G.D., 1979b. *Marine Bars and Nearshore Sedimentary Processes, Kouchibouguac Bay, New Brunswick, Canada, in Nearshore Sediment Dynamics and Sedimentation.* New York: John Wiley, pp. 123–150.

Holland, K.T.; Holman, R.A.; Lippmann, T.C.; Stanley, J., and Pland, N., 1997. Practical use of video imagery in nearshore oceanographic field studies. *Journal of Oceanic Engineering,* 22, 81–92.

Holman, R.A. and Bowen, A.J., 1982. Bars, bumps, and holes: models for the generation of complex beach topography. *Journal of Geophysical Research,* 87, 457–468.

Keulegan, G.H., 1948. An experimental study of submarine sand bars, Technical Memory 3, 40p., U.S. Army Corps of Engineering, Beach Erosion Board.

Lau, J. and Travis, B., 1973. Slowly varying Stokes waves and submarine longshore bars. *Journal of Geophysical Research,* 78, 4489–4497.

Lippmann, T.C. and Holman, R.A., 1990. The spatial and temporal variability of sand bar morphology. *Journal of Geophysical Research,* C7, 11575–11590.

Moore, L.J.; Sullivan, C., and Aubrey, D.G., 2003. Interannual evolution of multiple longshore sand bars in a mesotidal environment, Truro, Massachusetts, USA. *Marine Geology,* 96, 127–143.

Munoz-Perez, J.J.; Medina, R., and Tejedor, B., 2001. Evolution of longshore beach contour lines determined by the EOF method. *Scientia Marina,* 65(4), 393–402.

Ruessink, B.G. and Terwindt, J.H.J., 2000. The behavior of nearshore bars on the time scale of years: a conceptual model. *Marine Geology,* 163, 289–302.

Ruessink, B.G.; Van Enckevort, I.M.J., and Aarninkhof, S.G.J., 2002. Nearshore bar crest location quantified from time-averaged X-band radar images. *Coastal Engineering,* 45, 19–32.

Shenoi, S.S.C.; Murty, C.S., and Veerayya, M., 1987. Monsoon-induced seasonal variability of sheltered versus exposed beaches along the west coast of India. *Marine Geology,* 76, 117–130.

Short, A.D., 1975. Multiple offshore bars and standing waves. *Journal of Geophysical Research,* 80, 3838–3840.

Short, A.D., 1979. Three dimensional beach-stage model. *Journal of Geology,* 87, 553–571.

Solow, A.R., 1987. Testing for climatic change: an application of the two phase regression model. *Journal of Climate and Applied Meteorology,* 56, 1401–1405.

Sunamura, T. 1988. *Beach Morphologies and Their Change, in Nearshore Dynamics and Coastal Processes: Theory, Measurement, and Predictive Models.* Tokyo: University of Tokyo Press, pp. 136–152.

Van Enckevort, I.M.J. and Ruessink, B.G., 2001a. Effects of hydrodynamics and bathymetry on video estimates of nearshore sandbar position. *Journal of Geophysical Research,* 6, 16969–16979.

Van Enckevort, I.M.J. and Ruessink, B.G., 2001b. Alongshore uniform and nonuniform bar crest change. *In: Proceedings of Coastal Dynamics '01* (New York, ASCE), pp. 656–665.

Van Enckevort, I.M.J. and Ruessink, B.G., 2003.Video observations of nearshore bar behaviour. Part 1: alongshore uniform variability. *Continental Shelf Research,* 23, 501–512.

Wallace, J.W., 1972. Empirical orthogonal representation of time series in the frequency domain, part 1: theoretical consideration. *Journal of Applied Meteorology,* 11, 887–892.

Wijnberg, K.M. and Terwindt, J.H.J., 1995. Extracting decadal morphological behavior from high-resolution bathymetric surveys along the Holland coast using eigenfunction analysis. *Marine Geology,* 126, 301–330.

Winant, C.D.; Inman, D.L., and Nordstotorm, C.E., 1975. Description of seasonal beach changes using empirical eigenfunctions. *Journal of Geophysical Research,* 80(15), 1979–1986.

Wright, L.D.; Chappell, J.; Thom, B.G.; Bradshaw, M.P., and Cowell, P., 1979. Morphodynamics of reflective and dissipative beach and inshore systems: Southeastern Austration. *Marine Geology,* 32, 105–140.

Wright, L.D. and Short, A.D., 1984. Morphodynamic variability of surf zones and beaches: a synthesis. *Marine Geology,* 56, 93–118.

Yang, G.R.; Li, C.C.; Luo, Z.R., and Ying, Z.F., 1995. *Research on the Coastal Morphodynamic Science and its Application into the Harbor Restruction in South China.* Zhongshan, China: Zhongshan University Press, pp. 207–242 (in Chinese).